Preprints (www.preprints.org) | NOT PEER-REVIEWED | Posted: 7 February 2020 doi:10.20944/preprints202002.0094.v1

Mathematical Modelling of Pyrolysis of Hardwood (Acacia)

Alok Dhaundiyal[1], Suraj B. Singh[2], Istvan Backsai[3]

[1, 3]*Institute of Process Engineering, Szent Istvan University, Godollo, Hungary.*

[2]*Govind Ballabh Pant University of Agriculture and Technology, Pantnagar, Uttarakhand, India.*

***Abstract* -- This paper emphasises on the analogous modelling of hardwood (Acacia) pyrolysis. The effect of physical characteristics of hardwood chips on the pyrolysis is examined through the conservation of solid mass fraction of biomass. The chip size of G30 and G50 are used in the pyrolysis reactor. In the analogous situation, the fixed bed is assumed to be a wooden slab with a porosity equivalent to the voidage of bed. The bulk density, the length of the bed and the porosity are some of the physical attributes of a fixed bed used to determine the variation of solid mass of the hardwood across the fixed bed. The four-temperature sensors separated from each other by 80 mm are used to determine the temperature along the length of the pyrolysis unit. The heating element of 2 kWe is used to initiate the pyrolysis of biomass. The experiments are conducted in three different stages. The ONORM standard chips, G30 and G50, and the combination of them are separately pyrolysis to determine the validity of a model for different sizes of chips. The proposed model is also used to establish the relationship between the kinetics of pyrolysis and decomposition of the hardwood.**

***Keywords* -- Pyrolysis, hardwood chips, heat transfer, physical parameters, kinetics parameters**

Abbreviation

L	Equivalent length to the fixed bed	m
L_c	Equivalent length of the shrinking bed	m
G	Geometric parameter	m^{-1}
B	Biot number	
ρ_s	Density of solid mass	kg m^{-3}
T_g	Temperature of volatile gas	$^{\circ}C$
T_s	Temperature of solid mass	$^{\circ}C$
ε	Voidage of bed	
h_s	Internal energy of the solid mass	kJ/ kg
k_s	Thermal conductivity	kW m^{-1} K^{-1}
E	Apparent Activation energy	kJ/kg
A	Frequency factor	min^{-1}
Nu	Nusselt number	
θ_0	Temperature difference between solid and volatile gas	$^{\circ}C$
α_s	Thermal diffusivity of solid	m^2 s^{-1}
G30	Standard wooden chip size	mm
G50	Standard wooden chip size	mm
m	Mass of hardwood	g
P	Perimeter of slab	m
A	Cross-sectional area of slab	m^2

1. INTRODUCTION

Pyrolysis is one of the thermal degradation processes that take place in the presence of an inert atmospheric condition or in a limited supply of air. The pyrolysis in wood depends upon the physical structure of it, and it generally triggers at 200 °C and lasted until 450-500 °C. It plays a crucial role to understand an intrinsic mechanism of combustion of wood and sawdust since the released products, char and volatile matter, further undergo smouldering (glowing combustion) and flaming (light-emitting) combustion respectively to release thermal energy. Therefore, the important role of the pyrolysis is to understand the mechanism of combustion as well as establish a mathematical relationship between the physical and thermal parameters. The essential role of any model is to provide a computational inference for examining the system parameters and to recognise the relevance of system characteristics for knowing the behaviour of the system. Although the complexity of the thermo-chemical process makes the computational process cumbersome, yet it can be resolved using some cemented steps while formulating the proposed model. The pyrolytic decomposition of wood comprises the series of reactions, thus the altering thermal condition or characteristic of fuel may not only influence the rate of reaction but also the pathway of reactions.

In this article, the different perspective of modelling is proposed through the application of conservation of energy associated with solid biomass. The relationship between physical and thermal characteristics of wood and their influence on the decomposition process has been highlighted by the analogous scheme. However, the various modelling scheme pivoting around the kinetic aspect of the pyrolysis are summarised in the literature [1-6]. It is assumed that the fixed bed behaves like a porous wooden slab whose length sinks with time as a shrinking radius of the particle during combustion [7]. The impact of this study will help in determining the behaviour of biomass while physical characteristics of biomass alter with time and

Preprints (www.preprints.org) | NOT PEER-REVIEWED | Posted: 7 February 2020 doi:10.20944/preprints202002.0094.v1

temperature, and to establish an analogous scheme which is equivalent to a transformation of the fixed bed under the given thermal conditions. Moreover, the correlation between physical attribute and thermal properties can also be established.

2. MATERIAL AND METHODS

2.1. Modelling Scheme

Material characteristic has vital importance during the conceptual stage of modelling. Generally, the thermal parameters, diffusivity and thermal conductivity, directly influence the process of pyrolysis. The physical factor, bulk density, and temperature of material can easily be related to heat and mass transfer properties by the basic experiments. On the other hand, heat conduction through the porous medium varies with the direction of flow of heat across the biomass. So, the overall thermal conductivity is the summation of thermal conductivities of the air-void spaces and the solid biomass. Aforementioned process can be followed to measure the heat capacity and the heat transfer coefficient. Anisotropy of wood can be known through this fact that permeability of fluid along the grains is 10^4 times higher than across the grain; whereas thermal conductivity along the grain is twice over the thermal conductivity across the grain [8]. Furthermore, the effect of directional flow also decides the characterise of reaction pathways [8]. It is reported that the thermal conductivity of pyrolysed material is a linear function of thermal conductivity of the virgin wood and char, which is related to an instantaneous density of wood. Moreover, it is noticed that the temperature and mass loss predictions are sensitive to the assumed value for the thermal conductivity of char [9]. However, the measurement of thermal parameters at very high temperature is quite complicated due to chemical alteration and the drastic variation in physical properties makes computational work much complex.

Some heat and mass transfer models, which combines the chemical kinetics with the application of heat transfer are proposed to determine the effect of thermal parameters on the thermo-kinetics of material [10]. One of such models, a volume reaction model, emphasises on the simultaneous heat and mass transfer in the particle [11. In the unreacted shrinking core model for high temperature [10], the reaction at an unreacted shrinking core of solid is initiated by the surrounded pyrolysed layer of material around it. The reaction takes place at the interface of these two solid regions, therefore the conduction mode plays a major to dissipate the thermal energy from the charred layer. The energy transferred during this autocatalytic process is subjected to vary with the temperature gradient and the radius of the unreacted core. The same energy is utilised to commence pyrolysis in the biomass. The produced gases formed during pyrolysis advances radially outward. The unsteady rise of temperature inside particles is a time function of porosity, which helps to distinguish the variation of internal energy change of the gas and solid. A gas-solid thermal equilibrium can only be maintained for the low velocity of fluid flow across material [12]. Furthermore, the fluid and solid matrix remain in the local thermal equilibrium for the high value of the Peclet number [13]. Another aspect of heat transfer is to determine the thermal profile required as an explanatory variable in the kinetic model. Thus, the information about the heat transfer parameters assists in evaluating the accuracy of the prediction of the overall model. Some other models have also incorporated the internal convective heat transfer and temperature dependent thermal conductivity [14, 15, 16]. In this study, a wooden slab, which is analogous to a fixed bed, is subjected to transfer heat across slab along the length, L. The schematic diagram of the assumed wooden slab is given in Fig. 1. As, in similitude, a model is simulated according to the protype or actual system, so is being carried out in this study. A fixed bed of biomass is geometrically simulated. Thus, the wooden slab is a geometrical similitude of the bed. The length of bed is 80 mm, so the equivalent length of bed with respect to G30 and G50 are derived by the algorithm. In actual situation porosity increases with time and temperature. But for the sake of simplicity of the model, the porosity has been kept constant. It is just like a parameter, not variable which can be changed, so an individual can test the model at different porosity. But for comparison, parameters are assumed to be fixed in modelling problem so that relative variation can be measured. The initial sample is constant. Its variation is being calculated with the help of the equivalent wooden slab.

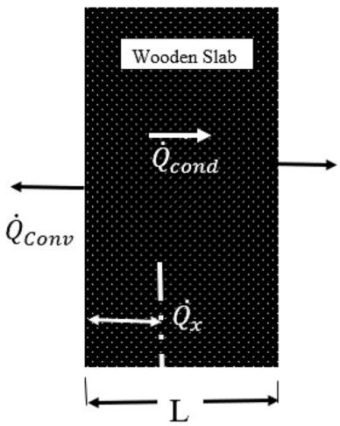

Fig. 1. The mode of heat transfer occurring during wood pyrolysis

Preprints (www.preprints.org) | NOT PEER-REVIEWED | Posted: 7 February 2020 doi:10.20944/preprints202002.0094.v1

According to the conservation of the solid energy (Eq. 1), the algebraic sum of the change of internal energy of solid (*I*), the heat conduction through the fixed bed (*II*), the internal connective heat transfer between fixed bed and the ambience (*III*), and the heat of reaction within the solid (*IV*) is equal to zero (Refer Appendix A.)

$$\underbrace{\Delta U}_{I} + \underbrace{\dot{Q}_{conduction}}_{II} + \underbrace{\dot{Q}_{convection}}_{III} - \underbrace{\Delta H_{heat\ of\ reaction}}_{IV} = 0 \quad (1)$$

Simplification of the Eq. (1) in time basis can be expressed as,

$$\frac{\partial\{h_s\rho_s(t)(1-\varepsilon)\}}{\partial t} - \left(k_s(1-\varepsilon)\frac{\partial T}{\partial x}\right)_{x=L} + \frac{\bar{h}}{(1-\varepsilon)}(\theta_0) - \frac{\partial\{C_p\rho_s(t)(1-\varepsilon)T\}}{\partial t} = 0 \quad (2)$$

where,

$$\theta_0 = \left(T_s - T_g\right) \text{ and } \quad G = \sqrt{\frac{h_s P}{k_s A}}$$

$$\frac{h_s}{k_s}\left(\frac{\partial\{\rho_s(t)(1-\varepsilon)\}}{\partial t}\right) - (1-\varepsilon)\left(G\frac{Sinh[G(x-L_c)]}{cosh[G(L-L_c)]} + \frac{\partial T_g}{\partial x}\right) + \frac{\overline{Nu}}{L}\frac{1}{(1-\varepsilon)}\left(\frac{cosh[G(x-L_c)]}{cosh[G(L-L_c)]}\right) - \frac{1}{\alpha_s}\frac{\partial\{T\}}{\partial t} = 0 \quad (3)$$

Integrate the Eq. (3) with respect to time, t, we get expression for mass losses during pyrolysis for the combination of G30 and G50 chips.

$$m_c(t) = 0.001\, m_c(t_0) - \Big[0.000864[L^2(-0.0045.L^2 + 0.267.L) - L_c^2(-0.0018L.L_c + 0.8013L + 0.00135L_c^2 - 0.534L_c)] + 0.000864\Big[G\{(L.L_c - 2 - L_c^2)sech\big(G(L-L_c)\big) - 1000L.tanh\big(G(L-l_c)\big)\} + 0.28\{L + (L-2L_c).sech\big(G(L-L_c)\big) - 2.tanh(G(L-L_c))\}\Big]\Big] \quad (4)$$

Similarly, the deduced expression for the mass losses whilst pyrolysis of hardwood chips, G30 and G50 are given by the Eq. (5) and Eq. (6) respectively.

$$m_{G30}(t) = 0.001\, m_{G30}(t_0) - \Big[0.032[L^2(0.3847L - 0.00068L^2) - L_c^2(0.00205L_c^2 + 1.154L - 0.00273LL_c - 0.7694L\_c)] + 0.032\Big[G\{(L.L_c - 2 - L_c^2)sech\big(G(L-L_c)\big) - 1000L.tanh\big(G(L-l_c)\big)\} + 0.28\{L + (L-2L_c).sech\big(G(L-L_c)\big) - 2.\tanh(G(L-L_c))\}\Big]\Big] \quad (5)$$

$$m_{G50}(t) = 0.001\, m_{G50}(t_0) - [0.00889[L^2(0.2208L - 0.00033L^2) - L_c^2\,(0.001L_c^2 - 0.441L_c + 0.662L - 0.00133LL_c)] + 0.00889\Big[G\{(L.L_c - 2 - L_c^2)sech\big(G(L-L_c)\big) - 1000L.tanh\big(G(L-l_c)\big)\} + 0.28\{L + (L-2L_c).sech\big(G(L-L_c)\big) - 2.\tanh(G(L-L_c))\}\Big] \quad (6)$$

The relationship between the rate of change of reactant and density of the wooden slab is given by Eq. (7)

$$\frac{dm}{dt} = -A.\exp(-E/RT)|\rho - \rho_{char}| \quad (7)$$

2.2. Experimental set-up

The experimental testing rig is situated at the National Agriculture Research and Innovation Centre, Hungary. The different size of the hardwood chips (G30 and G50) are used for the experimental purpose. The physio-chemical properties of hardwood are determined through physical and chemical analysers. To measure the extensive and intensive properties of the system, thermogravimetric, and the pressure and temperature sensors are retrofitted around the periphery of the pyrolysis reactor. The illustrative diagram of reaction is shown in Fig. 2. Thermocouple used for measuring the local temperature is 'K' type (Nickel-Chromium/ Nickel-Alumel). The weight sensor, which is separated by the insulating cover, is kept under the heating chamber. All the sensors are connected to the computer through a data logger. The volumetric rate of inert gas is controlled by a flow meter. The indirect heating element (Hertz-filament, Hungary) of 2 kWe is installed inside the reactor to initiate pyrolysis process of biomass. The grid material of heating chamber is made of 0.7 mm stainless steel, while the rock wool of 50 mm thickness is coated around the reactor. The core of the pyrolysis chamber is made up of 1.5 mm welded carbon steel. The inner diameter of reactor is 110 mm, whereas the outer diameter is 210 mm. The material used to fabricate the periphery of reactor is Aluminium. Elemental composition of the raw material is determined through CHN-S analyser. The analyser gets heated up to temperature of 1473 K for 30 mins. The helium gas is used as a carrier gas inside CHN-S analyser. The function of carrier gas is to carry away the product of combustion to different reduction columns. These tubes are placed in-between the combustion chamber and the signal-processing unit. The gases are separated into their constituents through purge or trap chromatography. After this process, each component is individually detected by a thermal conductivity detector (TCD). The product of combustion is absorbed in sequence; however, nitrogen does pass through the reduction columns. The physiochemical characteristic of hardwood (acacia) is illustrated in Table 1 (dry basis). The kinetic parameters are determined using eq. (7). The area under the predicted curves is evaluated through the MATLAB software. The integrated Eq.s (4), (5) and (6) are compared with the Eq. (7) and thus, the kinetic parameters are evaluated.

Preprints (www.preprints.org) | NOT PEER-REVIEWED | Posted: 7 February 2020 doi:10.20944/preprints202002.0094.v1

Table 1. The physiochemical characteristic of hardwood (dry basis)

C%	H%	N%	S%	O%	Ash %	H.H.V* (MJ/kg)	Bulk density (kg/m^3)	Material density (kg/m^3)
45.84	5.62	0.18	0.06	39.91	0.58	19.02	545	760

*-- Higher heating value

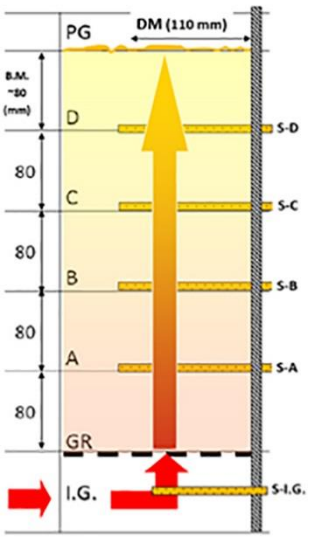

Fig. 2. Schematic diagram of pyrolysis reactor (S-A, S-B, S-C, S-D, Temperature sensors; S-I-G, thermogravimetric sensor; GR, grate material)

3. RESULTS AND DISCUSSION

An analogous model for hardwood pyrolysis is used to determine the effect of physical properties on decomposition of hardwood chips. Variation of the proposed geometrical parameter (G) on the mass loss curves is illustrated in Fig. 3. The geometrical parameter (G) is a dependant function of the thermal and geometric parameters of a wooden slab. However, the thermal properties are fixed for a particular material, hence it does not vary with a given condition. The dimension of slab is subjected to alter so that the effect of geometry of a pyrolysis bed on the mass loss variation can be examined. It is known through the proposed modelling scheme that the increasing value of G gets shifted the mass-loss curve upwards. It implies that the symmetrical slab allows more char production than that of the asymmetrical one. Moreover, the fractional reduction of the residual mass is relatively high due to asymmetricity. This is due to reason that a symmetrical slab lets the volatiles escape more quickly than that of an asymmetrical one, thus the thermal energy accompanied the released gas reduces the residence time of volatiles inside the matrix. Finally, it prevents autocatalytic reaction to occur inside the matrix, hence the large size chip helps to develop the large thermal gradient, and it causes local condensation of volatile. The similar attribute has also been reported for pyrolysis of a large particle [12, 17]. The thermal gradient is also affected by the geometry of slab. The thermal gradient across the wooden slab of the G50 chip is higher than that of the wooden slab of G30 chip. The value of the Biot number, B, varies from 7.49 to 10.32 for different size of hardwood chips (Table 2.), which implies that temperature gradient across the slab is non-uniform. It is also established from the experimental results that the non-uniform distribution of temperature across the fixed bed does exist and it affects the mass variation of hardwood chips with respect to time (Fig. 4). Moreover, to determine whether the proposed scheme can be extrapolated, it is necessary to examine the higher thermal regime, so that the application of the model can be demarcated.

Table 2. Parametric information of an equivalent wooden slab for the proposed model.

Hardwood Chips	R^2	L (m)	G (m^{-1})	B_i
G30	0.99	$0.0732 \leq L \leq 0.074$	$G \leq 3590$	7.49
G50	0.97	$0.095 \leq L \leq 0.108$	$G \leq 7161$	10.32
Combination (G30 and G50)	0.98	$0.085 \leq L \leq 0.0889$	$G \leq 5348$	8.84

Preprints (www.preprints.org) | NOT PEER-REVIEWED | Posted: 7 February 2020 doi:10.20944/preprints202002.0094.v1

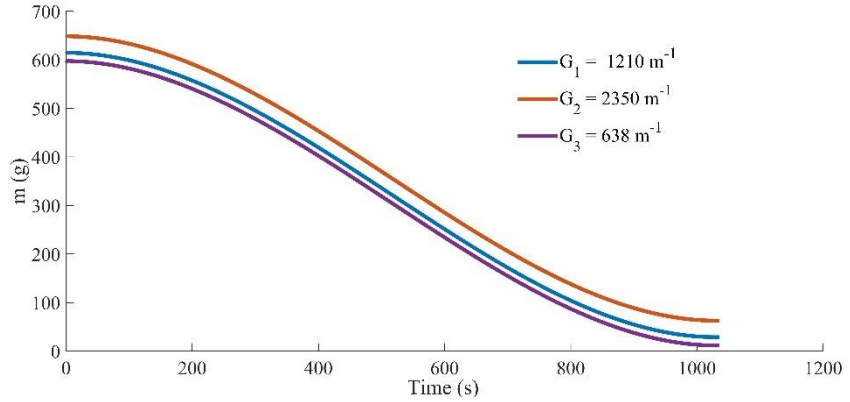

Fig. 3. The effect of the geometrical parameter 'G' on the numerical solution of pyrolysis of Hardwood chips.

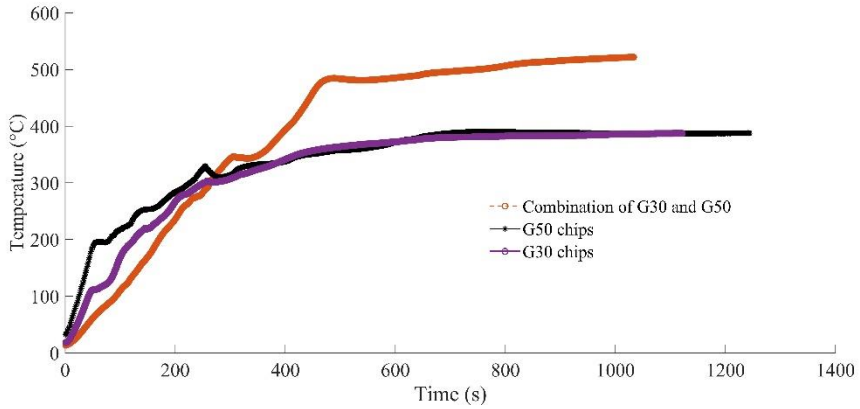

Fig. 4. Temperature distribution across pyrolysis bed of Hardwood.

The effect of equivalent length of slab is illustrated in Fig. 5. The length (*L*) of the slab, analogous to the height of the fixed bed of G30, G50, and combination of G30 and G50, affects the decomposition of the wooden slab at the beginning of pyrolysis. The increasing length of the wooden slab causes the mass-loss scale shifted upward which in turn decreases the rate of conversion of wood chips throughout the whole pyrolysis process. The relative change in the residual mass of wood due to variation of the equivalent length is lesser than the relative change of the initial mass of wood. It implies that the shrinkage of the wooden slab has a significant contribution to increase the convective heat transfer resistance across the wooden slab, thus the conversion rate is nearly the same for the varying size of wooden slab. It is noted that the same characteristics has been found for G30, G50 and the combination of both.

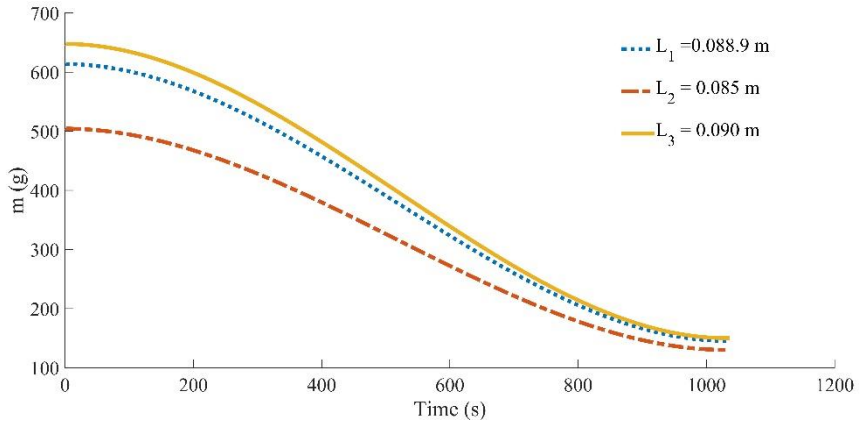

(a)

Preprints (www.preprints.org) | NOT PEER-REVIEWED | Posted: 7 February 2020 doi:10.20944/preprints202002.0094.v1

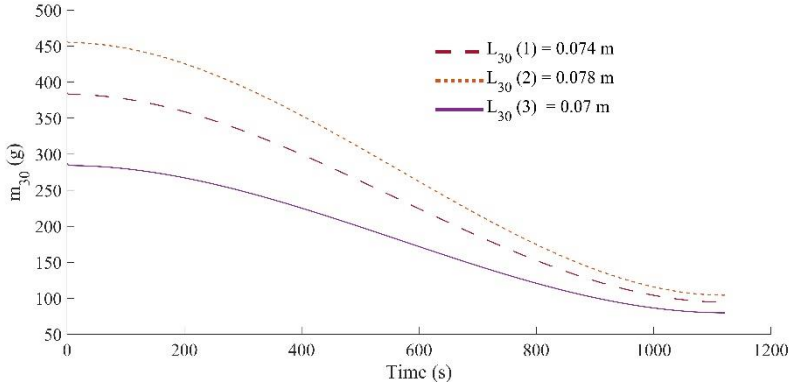

(b)

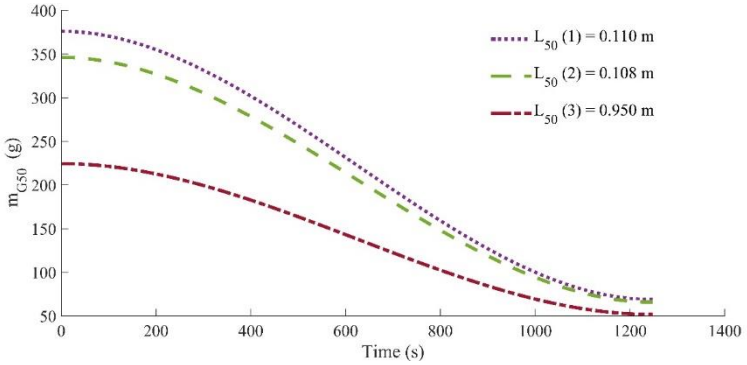

(c)

Fig..5. The behaviour of mass loss curve with respect to the equivalent length of slab, L.

The effect of porosity on the numerical solution is depicted in Fig. 6. The porosity is proportional to the volume fraction of the air void and solid mass. It can be seen through the predicted solution that the increasing fraction of porosity of air-void makes the mass-loss curve shifted downward at the beginning of pyrolysis. The conversion rate tends to be more uniform as the porosity increases, therefore it can be inferred that the fluid resistance to the volatile content increases. The resistance is relatively high in the large wooden slab; thus, the size of wooden slab may influence the extent of the secondary pyrolysis reactions as well as the yield of char through mass transfer. The direction of flow of heat perpendicular to the grain orientation also increases the residence time of pyrolysis gases and supports the autocatalytic reactions [8]. The experimental plot of mass-loss of hardwood chips is illustrated in Fig. 7. The similar characteristic has been observed through the proposed model. The decomposition curve of hardwood chip, G50, has relatively linear attribute at the onset of pyrolysis that shows thermal gradient across the fixed bed is larger than that of the fixed bed of G30 chips. Therefore, for the similar temperature interval, the domain of devolatisation is relatively extended for the large particle.

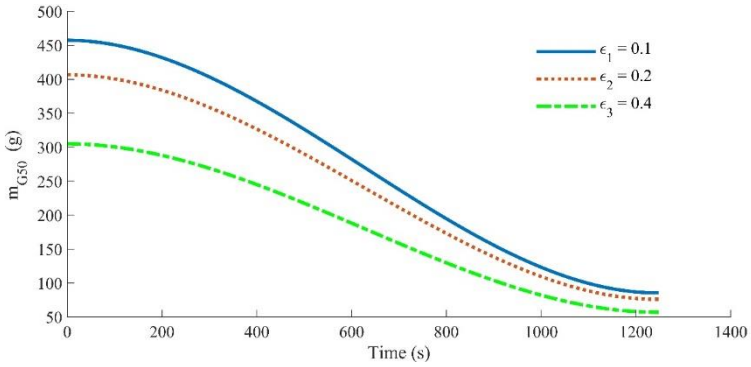

Fig. 6. The effect of porosity (ϵ) on the numerical solution of hardwood pyrolysis.

Preprints (www.preprints.org) | NOT PEER-REVIEWED | Posted: 7 February 2020 doi:10.20944/preprints202002.0094.v1

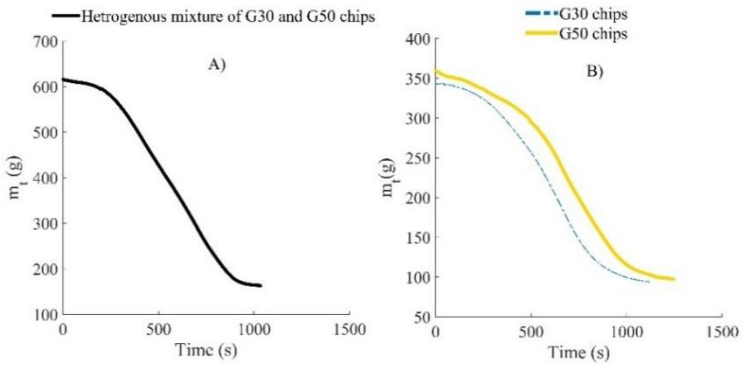

Fig. 7. Experimental plot of mass loss curves of different sized chips (G30 and G50) (A: combination of G30 and G50. B: G30 and G50 chips)

Comparison of the predicted solution for different sizes of the wooden slab with the experimental data is demonstrated in Fig. 8. It is clearly visible that the predicted solution provided the good correlation with the experimental curve. The assumption of the fixed bed as a wooden slab with the conversation of mass in pyrolysis problem of hardwood depicts that the residual mass, range of devolatisation, the convective resistance, the residence time of volatile in the matrix, and the effect on the conversion rate are highly influenced by physical characteristic of fuel. The predicted solution has good agreement at the initial stage of pyrolysis and the difference between residual masses of predicted and experimental is marginally low. On the other hand, the proposed model for G30 and G50 chips is depicted in Fig. 8 (b, c). Here, the numerical solution for G50 has shown a slight deviation in the residual mass, whereas the deviation of the residual mass for G30 is relatively low. This may be due to either non-uniformity of temperature gradient or the structural effects (surface cracks or longitudinal channelling), which occur due to the sudden drop of pressure inside the slab that leads to alter the heating characteristic of biomass.

The kinetic constants evaluated for different size of chips is shown in Table 3. The estimated value of activation energy is compared with the different species of wood and it is within permissible range of variation [18,19, 20]. The activation energy for hardwood (acacia) varies from 73.5 kJ mol^{-1} to 88.48 kJ mol^{-1}; whereas the frequency factor, 1.02 x 10^4 min^{-1} to 1.27 x 10^4 min^{-1}. The detailed information is given in Table 3. It is found that the size variation of wooden slab also affects the kinetic study of pyrolysis, however the range of temperature used for experimental purpose has a major role in determining the kinetic parameters. The difference between the kinetic parameters of wooden slabs of G30 and G50 chips is marginally narrow. The bulk density of bed and the porosity play a significant role to determine the apparent activation energy. It implies that the kinetic constants as well as the heat of reaction, before and after the breaking point of wood, differ from each other [21]. It is noted that the Monte Carlo is implemented to measure the kinetic parameters [22].

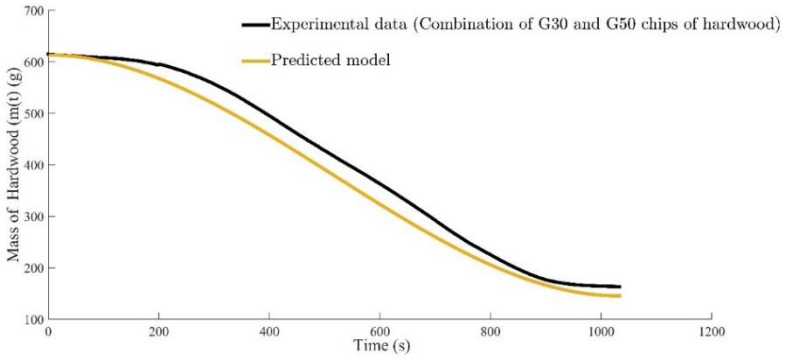

(a)

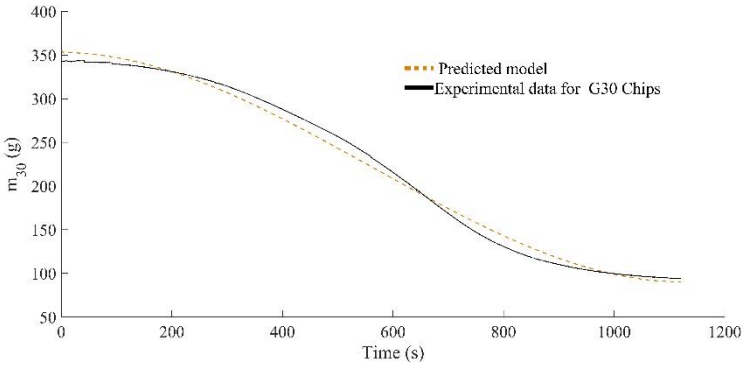

(b)

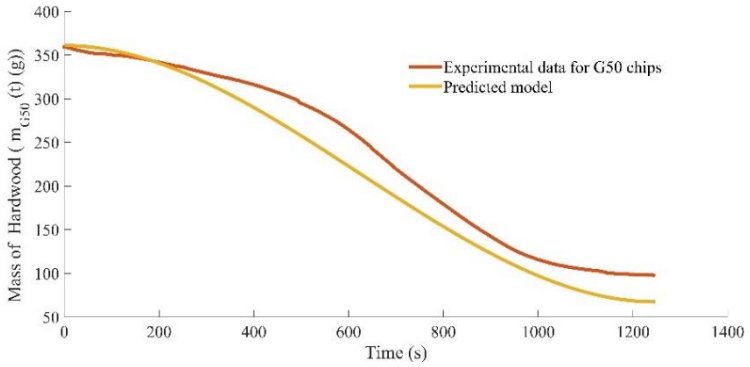

(c)

Fig. 8. Comparison of experimental data with the predicted solution for different combination of Hardwood chips.

Table 3. Kinetic constants for Hardwood (Acacia)

Area under curves	Chip Size	Activation Energy (kJ mol^{-1})	Frequency factor (min^{-1}.)	Activation Energy (kJ mol^{-1}) [18, 19]
148330 sq. Unit	G30	73.5	1.20 x 10^4	71 (Beech saw dust)
190940 sq. Unit	G50	74	1.06 x 10^4	125.4 (Softwood)
256610 sq. Unit	Combination	88.48	1.27 x 10^4	85.69 (Hardwood)

4. CONCLUSION

Modelling of pyrolysis of hardwood (Acacia) pivoted around the analogous model, which is equivalent to the fixed bed of pyrolysis reactor. The effect of physical characteristic of ONORM the Austrian standard for wood chip on the proposed model is examined. It is found that the equivalent length of wooden slab for G30 should vary from 73 to 74 mm, whereas it is relatively large for G50 and the combination of both of them. The wooden slab of 95 to 108 mm is suitable to simulate the result for G50 chips. On the other hand, it is 85 mm to 89.5 mm for combination of both. The results simulate through the proposed model provides the good correlation with experimental results. Moreover, the kinetic constants for hardwood is found to vary from 73.5 kJ mol^{-1} to 88.48 kJ mol^{-1}, which also lie within a permissible range of variation of activation energy for different species of wood. The Biot number for the wooden slab varies from 7.49 to 10.49, which implies that the temperature gradient has non-uniformity across the wooden slab. Moreover, the variation of bulk density of bed with respect to time also influence the thermo-kinetics of hardwood. It is concluded that kinetic constants, before and after the breakage point of wood, may differ from each other. The limiting factor of this analysis focuses on the resistance offers to the flow of fluid and the surface of the wooden slab. The convection resistance must be low and conduction resistance should be high, and it is clearly depicted by the Biot number. The decrease in the convection resistance must be higher than the increase in the conduction resistance for better correlation between the experimental and the mathematical model.

REFERENCES

[1] Dhaundiyal, A., Singh,S.B., Hanon , Schrempf, N. (2018) 'Clayton Copula as an Alternative Perspective of Multi-Reaction Model', *Environmental and Climate Technologies*, 22(1), pp. 83–106. doi: 10.2478/rtuect-2018-0006.
[2] Dhaundiyal, A., Singh, S. B. and Hanon, M. M. (2018) 'Study of distributed activation energy model using bivariate distribution function, f (E1, E2)', *Thermal Science and Engineering Progress*. doi: 10.1016/j.tsep.2018.01.009.
[3] Dhaundiyal, A. *et al.* (2018) 'Determination of Kinetic Parameters for the Thermal Decomposition of Parthenium hysterophorus', *Environmental and Climate Technologies*, 22(1), pp. 5–21. doi: 10.1515/rtuect-2018-0001.
[4] Cai, J. and Liu, R. (2008) 'New distributed activation energy model: Numerical solution and application to pyrolysis kinetics of some types of biomass', *Bioresource Technology*, 99(8), pp. 2795–2799. doi: 10.1016/j.biortech.2007.06.033.
[5] Dhaundiyal A, Abdulrahman TM and Laszlo T. (2018) 'Thermo-kinetics of Forest Waste Using Model-Free Methods', in *Universitas Scientiarum*, pp. 465–495. doi: 10.11144/Javeriana.SC23-3. tofw.
[6] Mani, T., Murugan, P. and Mahinpey, N. (2009) 'Determination of distributed activation energy model kinetic parameters using simulated annealing optimization method for nonisothermal pyrolysis of lignin', *Industrial and Engineering Chemistry Research*. doi: 10.1021/ie8013605.
[7] Scott Fogler, H. (1987) 'Elements of chemical reaction engineering', *Chemical Engineering Science*, 42(10), p. 2493. doi: 10.1016/0009-2509(87)80130-6.
[8] Roberts, A. F. and Clough, G. (1963) 'Thermal decomposition of wood in an inert atmosphere', *Symposium (International) on Combustion*, 9(1), pp. 158–166. doi: 10.1016/S0082-0784(63)80022-3.
[9] Kung, H. C. (1972) 'A mathematical model of wood pyrolysis', *Combustion and Flame*, 18(2), pp. 185–195. doi: 10.1016/S0010-2180(72)80134-2.
[10] Maa P.S. and Bailie R.C. 1973. Influence of Particle Sizes and Environmental Conditions on High Temperature Pyrolysis of Cellulosic Material -I (Theoretical) , *Combustion Science and Technology* 7: 257-269.
[11] Fan L.T., Fan L.S., Miyanami K., Chen T.Y. and Walawender P. 1977. Can. J. Chem Engg. 55 : 47-53.
[12] Chan, W. C. R., Kelbon, M. and Krieger, B. B. (1985) 'Modelling and experimental verification of physical and chemical processes during pyrolysis of a large biomass particle', *Fuel*, 64(11), pp. 1505–1513. doi: 10.1016/0016-2361(85)90364-3.
[13] Romagnosi, L. *et al.* (2013) 'Pyrolysis in porous media: Part 1. Numerical model and parametric study', *Energy Conversion and Management*, 68, pp. 63–73. doi: 10.1016/j.enconman.2012.12.023.

[14] Matsumoto, T., Fujiwara, T. and Kondo, J. (1969) 'Nonsteady thermal decomposition of plastics', in *Symposium (International) on Combustion*, pp. 515–524. doi: 10.1016/S0082-0784(69)80433-9.

[15] Sadhukhan, A. K., Gupta, P. and Saha, R. K. (2009) 'Modelling of pyrolysis of large wood particles', *Bioresource Technology*, 100(12), pp. 3134–3139. doi: 10.1016/j.biortech.2009.01.007.

[16] Polesek-Karczewska, S. and Kardaś, D. (2015) 'Prediction of thermal behavior of pyrolyzed wet biomass by means of model with inner wood structure', *Journal of Thermal Science*, 24(1), pp. 82–89. doi: 10.1007/s11630-015-0759-1.

[17] Bamford, C. H., Crank, J. and Malan, D. H. (1946) 'The combustion of wood. Part I', Mathematical Proceedings of the Cambridge Philosophical Society, 42(2), pp. 166–182. doi: 10.1017/S030500410002288X.

[18] Di Blasi, C. (1993) 'Modeling and simulation of combustion processes of charring and non-charring solid fuels', Progress in Energy and Combustion Science, pp. 71–104. doi: 10.1016/0360-1285(93)90022-7.

[19] Lim, S. M. and Chew, M. Y. L. (2005) 'Compensation effects in the non-isothermal pyrolysis of wood', in Fire Safety Science, pp. 1109–1120. doi: 10.3801/IAFSS.FSS.8-1109.

[20] Dhaundiyal, A. and Toth, L. (2020) 'Modeling of Hardwood Pyrolysis Using the Convex Combination of the Mass Conversion Points', *Journal of Energy Resources Technology, Transactions of the ASME*. doi: 10.1115/1.4045458.

[21] Tinney, E. R. (2007) 'The combustion of wooden dowels in heated air', Symposium (International) on Combustion, 10(1), pp. 925–930. doi: 10.1016/s0082-0784(65)80235-1.

[22] Dhaundiyal, A. *et al.* (2019) 'Application of Monte Carlo Simulation for Energy Modeling', *ACS Omega*, 4(3), pp. 4984–4990. doi: 10.1021/acsomega.8b03442.

Appendix A.

The modelling of hardwood pyrolysis assumes that the analogous wooden slab has the same voidage as the fixed bed of hardwood. The material is assumed to be isotropic, no heat generation within the slab, uniform heat transfer coefficient over the wooden slab and negligible radiation. The correlation between the fixed bed height and temperature of volatile is given by Eq. A.1 and Eq. A.2

$$T_g = 0.0041x^2 - 2.3083x + 482.22\ (G30) \quad \text{(A.1)}$$

$$T_g = 0.002x^2 - 1.3251x + 434.42\ (G50) \quad \text{(A.2)}$$

The shrinking bed follows the concept of the shrinking core model [7].

$$-\frac{dx}{dt} = \frac{D_e C_A}{\varepsilon \rho_s}\left(\frac{1}{x-\frac{x^2}{L}}\right) \quad \text{(A.3)}$$

After solving the differential Eq. (A.3), we get

$$L_c \sim \sqrt{\frac{1}{3}\left(1 - \frac{6D_e \Delta t C_A}{\varepsilon \rho_s L^2}\right)} \quad \text{(A.4)}$$

Here – C_A, concentration; D_e, effective diffusivity; ε, voidage

The effective values of thermal conductivity and thermal heat capacity are determined through Eq. (A.5) and Eq. (A.6)

$$\rho_b C_p = (1-\varepsilon)\rho_s C_s + \varepsilon \rho_g C_g \quad \text{(A.5)}$$

$$k_p = \boldsymbol{\varepsilon} k_g + (1-\varepsilon)k_s \quad \text{(A.6)}$$

Here, subscript 'g' and 's' represents void space and solid part of fixed bed

The Eq. (6) is valid for solid layers parallel to flow of heat (the parallel distribution)

Table A.1 Parametric information of thermal properties

h	23 kW m^{-2} K^{-1}
k_s	0.226

Preprints (www.preprints.org) | NOT PEER-REVIEWED | Posted: 7 February 2020 doi:10.20944/preprints202002.0094.v1

C_A	0.429 mol/m^3	
α_s	0.000374 m^2/s	
D_e	G30	$4.74\ x\ 10^{-06}\ m^2/s$
	G50	$1.70\ x\ 10^{-04}\ m^2/s$